ARMY RESEARCH LABORATORY

Temporal Evolution of the LIBS Spectrum of Aluminum Metal in Different Bath Gases

by Thuvan N. Piehler, Frank C. DeLucia, Jr., Chase A. Munson, Barrie E. Homan, Andrzej W. Miziolek, and Kevin L. McNesby

ARL-TR-3371 **December 2004**

NOTICES

Disclaimers

The findings in this report are not to be construed as an official Department of the Army position unless so designated by other authorized documents.

Citation of manufacturer's or trade names does not constitute an official endorsement or approval of the use thereof.

Destroy this report when it is no longer needed. Do not return it to the originator.

Army Research Laboratory
Aberdeen Proving Ground, MD 21005-5066

ARL-TR-3371 **December 2004**

Temporal Evolution of the LIBS Spectrum of Aluminum Metal in Different Bath Gases

Thuvan N. Piehler, Frank C. DeLucia, Jr., Chase A. Munson, Barrie E. Homan, Andrzej W. Miziolek, and Kevin L. McNesby
Weapons and Materials Research Directorate, ARL

REPORT DOCUMENTATION PAGE	Form Approved OMB No. 0704-0188

1. REPORT DATE *(DD-MM-YYYY)*	2. REPORT TYPE	3. DATES COVERED (From - To)
December 2004	Final	15 August 2003–15 August 2004

4. TITLE AND SUBTITLE
Temporal Evolution of the LIBS Spectrum of Aluminum Metal in Different Bath Gases

5a. CONTRACT NUMBER

5b. GRANT NUMBER

5c. PROGRAM ELEMENT NUMBER

6. AUTHOR(S)
Thuvan N. Piehler, Frank C. DeLucia, Jr., Chase A. Munson, Barrie E. Homan, Andrzej W. Miziolek, and Kevin L. McNesby

5d. PROJECT NUMBER
AH80

5e. TASK NUMBER

5f. WORK UNIT NUMBER

7. PERFORMING ORGANIZATION NAME(S) AND ADDRESS(ES)
U.S. Army Research Laboratory
ATTN: AMSRD-ARL-WM-BD
Aberdeen Proving Ground, MD 21005-5066

8. PERFORMING ORGANIZATION REPORT NUMBER
ARL-TR-3371

9. SPONSORING/MONITORING AGENCY NAME(S) AND ADDRESS(ES)
ASEE
1818 N. Street N.W., Ste 600
Washington, DC 20036

10. SPONSOR/MONITOR'S ACRONYM(S)

11. SPONSOR/MONITOR'S REPORT NUMBER(S)

12. DISTRIBUTION/AVAILABILITY STATEMENT
Approved for public release; distribution is unlimited.

13. SUPPLEMENTARY NOTES

14. ABSTRACT

The spectral emission of gas phase aluminum (Al) and Al oxide was measured during and immediately after exposure of a bulk Al sample to a laser-induced spark produced by a focused, pulsed laser beam (Nd:YAG, 10 ns pulse duration, 35 mJ/pulse, $\lambda = 1064$ nm). The spectral emission was measured as a function of time after the onset of the laser pulse, and was also measured in different bath gases (air, N_2, O_2, and He).

15. SUBJECT TERMS
spectroscopy, laser, LIBS, aluminum

16. SECURITY CLASSIFICATION OF:			17. LIMITATION OF ABSTRACT	18. NUMBER OF PAGES	19a. NAME OF RESPONSIBLE PERSON
a. REPORT	b. ABSTRACT	c. THIS PAGE			Thuvan Piehler
UNCLASSIFIED	UNCLASSIFIED	UNCLASSIFIED	UL	30	19b. TELEPHONE NUMBER (*Include area code*) 410-306-0884

Standard Form 298 (Rev. 8/98)
Prescribed by ANSI Std. Z39.18

Contents

List of Figures

List of Tables

1. Introduction

Aluminum (Al) is a common ingredient of explosives and propellants. In explosives, Al is used to augment air blast, raise reaction temperature, and create incendiary effects (*1*). In rocket propellants, Al is used to increase thermal energy and elevate the flame temperature (*2*). A proposed mechanism for the combustion of Al in O_2 follows(*3*):

$$Al\ (l) \rightarrow Al\ (g) \qquad \Delta H = 317.7\ kJ \qquad (1)$$

$$AlO + Al\ (l) \rightarrow Al_2O \qquad \Delta H = -224.0\ kJ \qquad (2)$$

$$Al\ (g) + O_2 \rightarrow AlO + O \qquad \Delta H = 6.53\ kJ \qquad (3)$$

$$Al\ (g) + O + M \rightarrow AlO + M \qquad \Delta H = -492.1\ kJ \qquad (4)$$

$$AlO + O_2 \rightarrow AlO_2 + O \qquad \Delta H = -78.6\ kJ \qquad (5)$$

$$AlO + AlO_2 \rightarrow Al_2O_3\ (l) \qquad \Delta H = -1557.2\ kJ \qquad (6)$$

$$Al_2O + O_2 \rightarrow Al_2O_3\ (l) \qquad \Delta H = -1562\ kJ \qquad (7)$$

For some explosive materials, Al may be used to tailor performance to specific needs. Measurements of relative amounts of Al metal and Al oxide (AlO) during explosions of energetic materials may provide insight into increasing the performance of Al-containing explosives. The experiments described here are a preliminary study of the application of laser-induced breakdown spectroscopy (LIBS) to this problem.

Although best known for high selectivity for metals analysis (*4*), LIBS has also been used to detect energetic materials (*5*), trace elements in liquids (*6*), organic compounds in ambient air (*7*), and some biological materials (*8*). In LIBS, a pulsed laser focused onto a target material converts some of the material into a plasma of ions and electrons, with temperatures that may approach 20,000 K (*9*). As the plasma cools, some of the energy is radiated as light. When measured using a spectrograph, the wavelengths of the emitted light are characteristic to the elemental components of the target, while the intensity of light over a given wavelength range may yield the proportion of that element within the target material (*10*). Additionally, the time evolution of the emission following the laser pulse may be used to identify certain chemical reactions occurring in the plasma as it cools.

In this report, we measure the emission from a laser-induced spark produced by focusing a pulsed Nd:YAG laser onto the surface of an Al rod. The emission is spectrally and temporally resolved, the effect of different bath gases (air, O_2, N_2, and He) on the emission is measured, and temperature and electron density are calculated.

2. Experimental

A schematic of the simple LIBS system used in this work is shown in figure 1. Briefly, a light pulse (~10 ns, 35 mJ per pulse) from an actively Q-switched Nd-YAG laser (Big Sky Laser Technologies Inc., Bozeman, MT) emitting at a wavelength of 1064 nm was focused by a 50-mm convex lens onto the surface of an Al rod. A Si-Si optical fiber (600-μm core diameter) collected the emission from the plasma spark. A lens was placed in front of the fiber so that the plasma spark was sufficiently defocused to eliminate any spatial effects. An echelle spectrometer (Catalina Scientific Corp., Tucson, AZ) fitted with a gated, intensified CCD camera (Andor Technology Com., Model DH 734-18-03) was used to measure the emitted light. The entire experiment, including background measurement, laser control, data acquisition, and data processing, was controlled by a laptop computer (Dell).

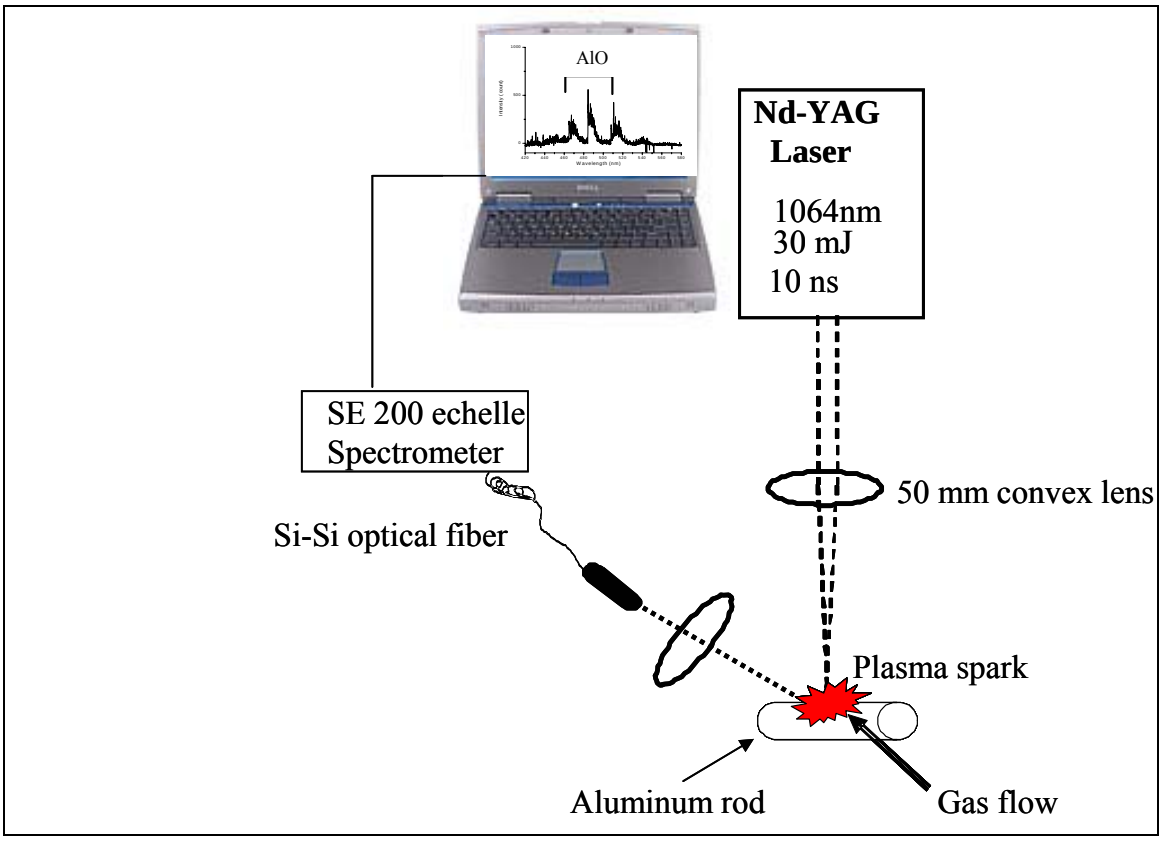

Figure 1. Schematic of the experimental setup used to measure LIBS spectra.

Prior to the measurement of each LIBS spectrum, a background spectrum was measured and subsequently subtracted from the sample spectral data. In an attempt to minimize errors due to shot to shot variations in the laser output power (~5%), each spectrum used in the data analysis is the average of 50 "single shot" spectra. For each LIBS spectrum measured, the Al rod was

repositioned so only a new sample was exposed to the laser-induced spark. To enable comparison with previous LIBS studies of Al (*11*), a detector gate width of 2 μs was used for these experiments. Detector gate delays (relative to the Q-switch of the Nd:YAG laser) ranged from 0 to 30 μs. The composition of Al rods used in this study was Al 91.4%, Cu 5.67%, Fe 1.28%, Li 1.11%, and minor constituents (Mg, Mn, Ti, and Zn percentage <0.5% by weight). Bath gases (N_2, O_2, and He) were obtained from Matheson and were used without any further purification. Typical flow rates were ~2 L/min. The gas flow was delivered via 4-mm I.D. Tygon tubing. The exit port of the tubing was ~5 mm from the location of the plasma volume.

3. Results and Discussion

3.1 Emission Spectra of an Al Rod in Air

The most intense regions of the Al rod LIBS spectrum (bath gas = air [ambient], gate width = 2 μs, gate delay = 20 μs) are shown in figures 2, 3, and 4. The first spectral window (figure 2) from 300 to 420 nm includes emission from gas phase aluminum (Al I) at wavelengths of 308.34, 309.44, 394.56, and 396.26 nm. The second spectral window (figure 3; 420–580 nm) includes emission from the gas phase molecular species AlO, with the most intense emission near 484.58 nm. The third spectral window (figure 4; 740–760 nm) includes emission from gas phase aluminum (Al II) at a wavelength of 747.14 nm. For Al combustion in air, previous investigators have suggested that above the melting point of Al_2O_3 (2315 K) (*12*), the Al species with highest partial pressures are Al and AlO.

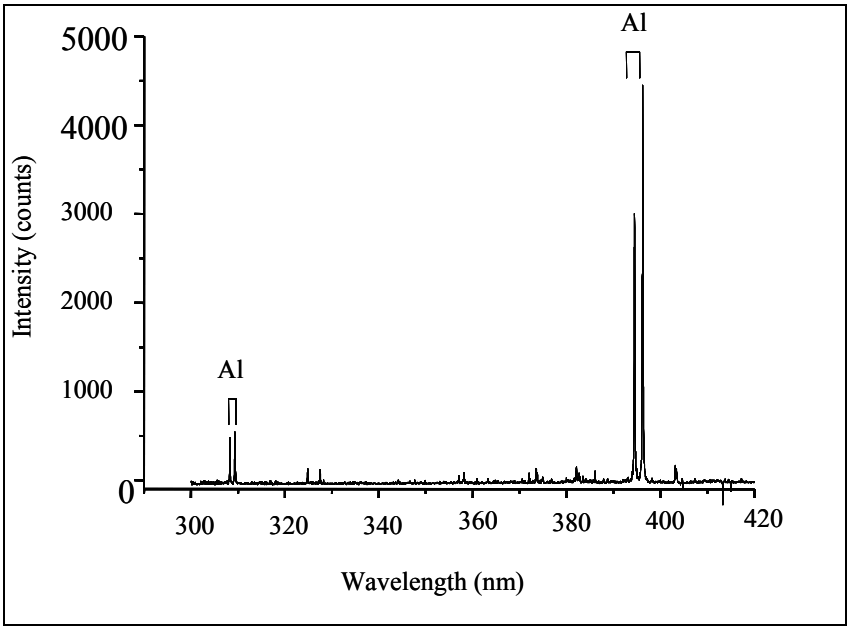

Figure 2. A portion of LIBS spectrum of an Al rod in air with a 20-μs gate delay and 2-μs gate (300–420-nm region).

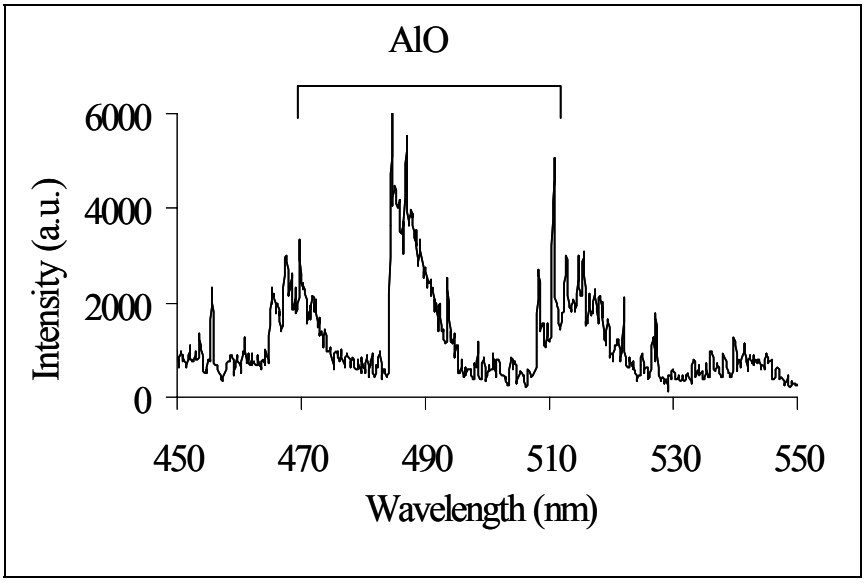

Figure 3. A portion of LIBS spectrum of an Al rod in air with a 20-μs gate delay and 2-μs gate (450–550-nm region).

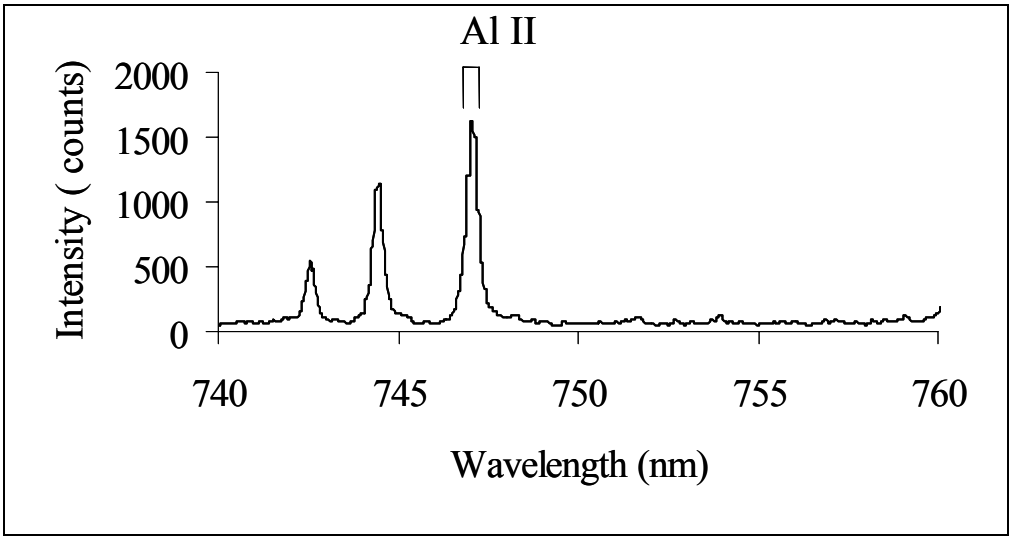

Figure 4. A portion of LIBS spectrum of an Al rod in air with a 20-μs gate delay and 2-μs gate (740–760-nm region).

3.2 Temporal Evolution of Al and AlO Emission

Figure 5 shows the LIBS spectrum of an Al rod in air at various gate delays (gate width = 2 μs). As seen in figure 5, the Al I line (396.2 nm) reaches its maximum intensity in air ~5 μs after the laser pulse. The band from AlO emission (484.4 nm) reaches its maximum intensity ~20 μs after the laser shot. This is qualitatively consistent with the combustion mechanism for Al in oxygen, outlined in reactions 1–7 earlier.

LIBS spectra of the Al rod (measured from 350 to 580 nm) at various gate delays (gate width = 2 μs) for the bath gases O_2, He, and N_2 are shown in figures 6, 7, and 8, respectively. For comparison, the peak intensities of the Al I line in each figure have been normalized. It is worth noting that the emission near 484 nm (from AlO) in figure 7 (He bath gas) and figure 8 (N_2 bath gas) is vanishingly small compared to the emission near 484 nm in figure 5 (air bath gas) and figure 6 (O_2 bath gas).

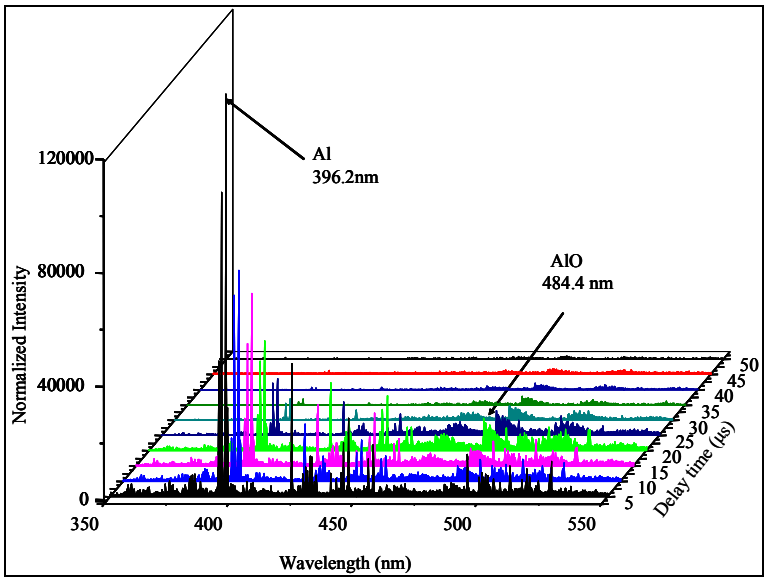

Figure 5. LIBS spectrum of an Al rod in air, at various gate delays. The gate pulse width is 2 μs.

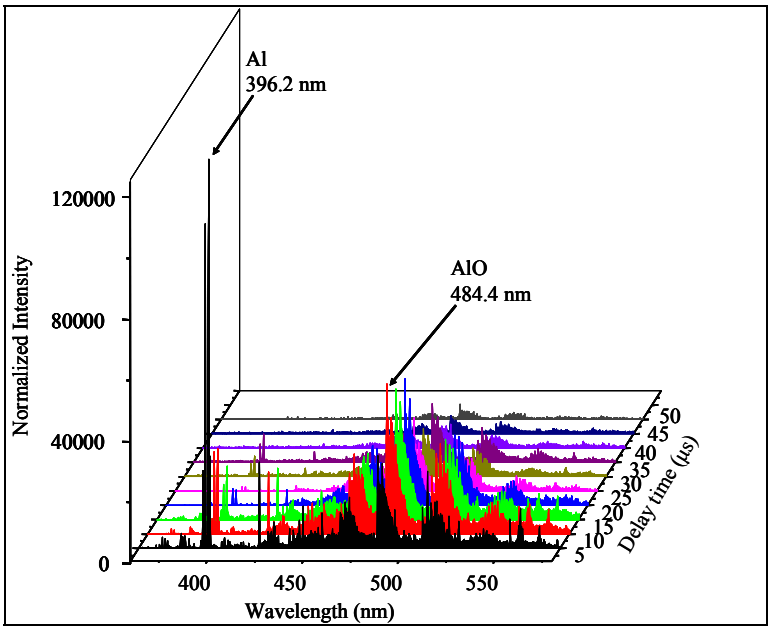

Figure 6. Temporal emission evolution of Al LIBS in O_2. The gate pulse width is 2 μs.

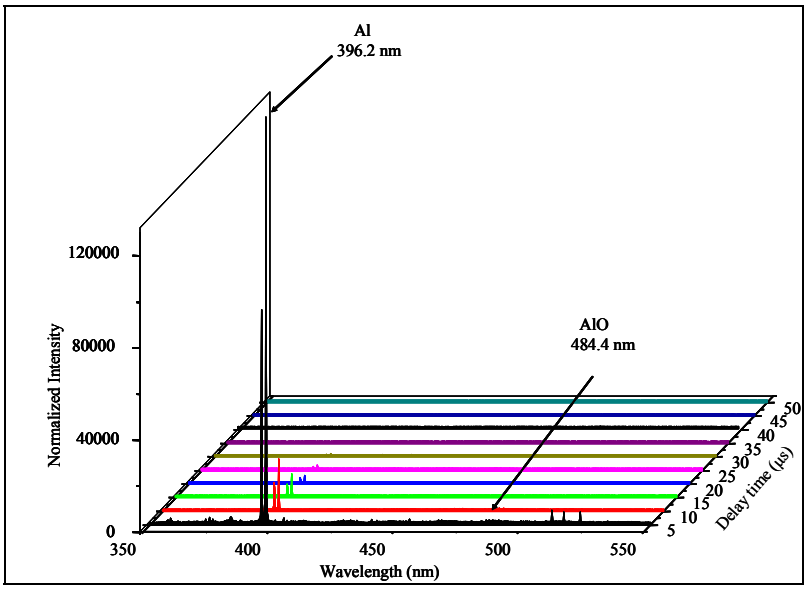

Figure 7. Temporal emission evolution of Al LIBS in He. The gate pulse width is 2 μs.

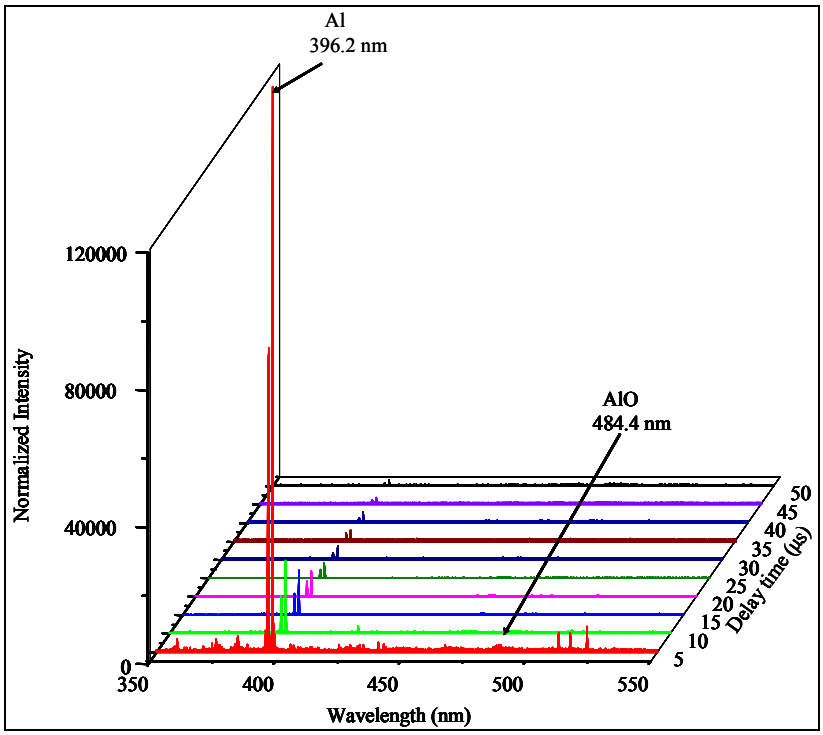

Figure 8. Temporal emission evolution of Al LIBS in N_2. The gate pulse width is 2 μs.

Figure 9 shows that the decrease in Al emission (396 nm) with time appears exponential. Figure 10 shows a pseudo-first-order plot of logarithm of intensity at 396 nm vs. time. From this plot, the deactivation of Al (fastest to slowest) as a function of bath gas is O_2~He>air>N_2. Figures 11 and 12 (expanded by a factor of 10,000) show the maximum emission intensity of the AlO band

near 484 nm as a function of time for reactive (air and O_2) and nonreactive (He and N_2) bath gases, respectively. Figure 11 shows that the maximum emission from AlO occurs 10 μs after the laser pulse in the pure O_2 atmosphere, while the intensity in air reached a maximum 20 μs after the laser pulse. Therefore, we believe the main source of AlO emission in bath gases of O_2 and air is AlO formed by the reaction of Al (g) with ambient O_2, analogous to reactions 3 and 4 for the combustion of Al in O_2. This is also supported by the increase in AlO emission as the bath gas is changed from air (figure 5) to O_2 (figure 6).

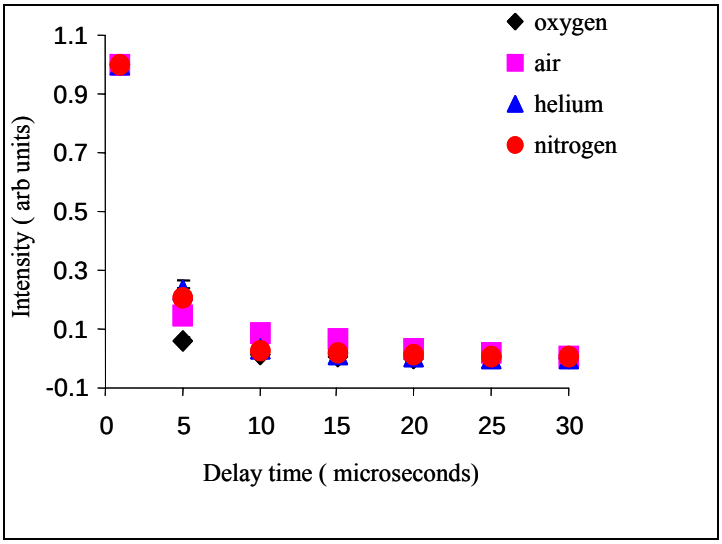

Figure 9. Comparison of time evolution of emission intensity for Al (396-nm) LIBS signal in air, He, N_2, and O_2 with a 2-μs gate pulse width.

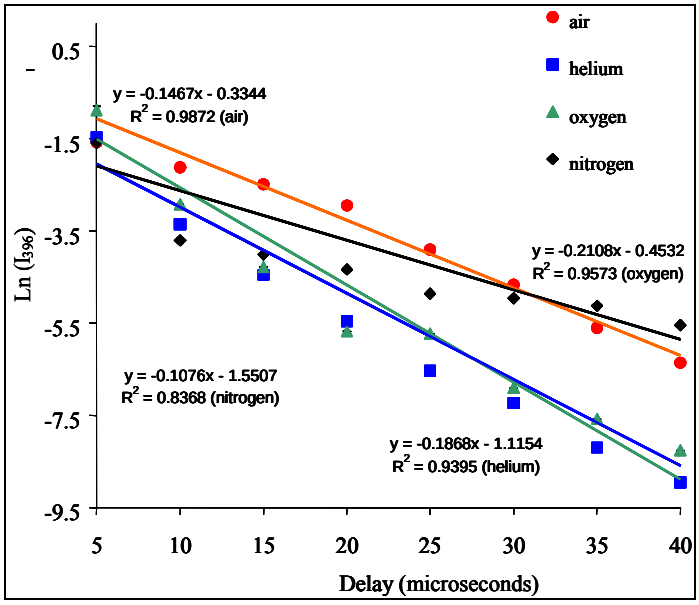

Figure 10. A plot of logarithm of intensity at 396 nm vs. time for the different bath gases used in these experiments.

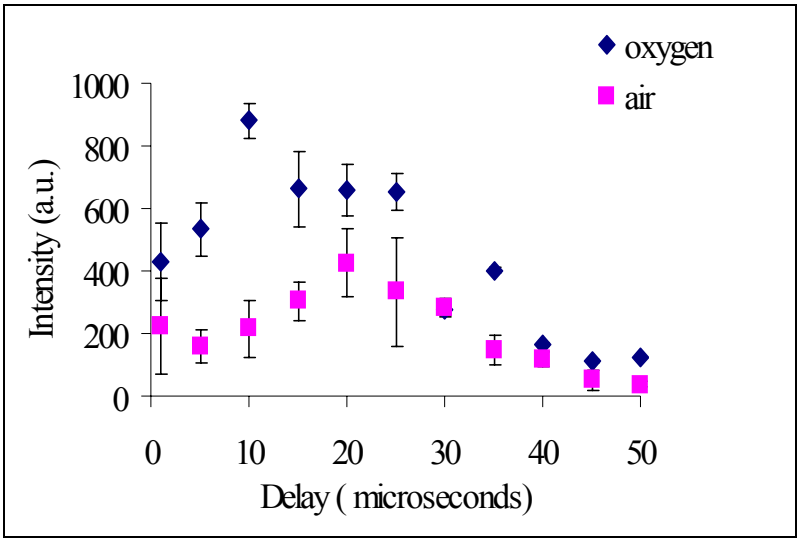

Figure 11. The maximum emission intensity of the AlO band near 484 nm as a function of time for the bath gases air and O_2.

Figure 12 shows that, in the absence of ambient O_2, the temporal behavior of the AlO emission is similar to that of the Al emission; i.e., the temporal behavior of the AlO emission in the unreactive bath gases is similar to emission from material (Al) native to the Al rod. Therefore, we believe the source of the AlO emission in the absence of ambient O_2 is the Al_2O_3 layer on the Al metal.

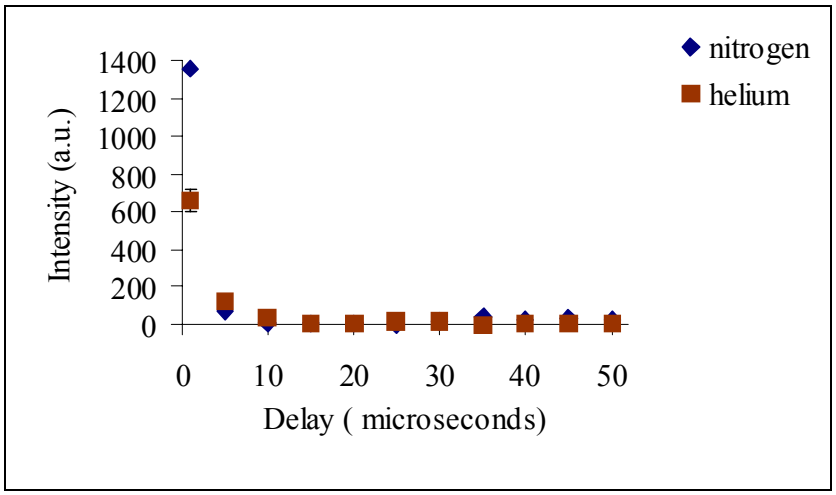

Figure 12. The maximum emission intensity of the AlO band near 484 nm as a function of time for the bath gases He and N_2.

3.3 Temperature Calculations

For the temperature calculations reported, we assume that for the gate width used (2 μs), the time rate of change of the plasma temperature is small, and that light emission collected and analyzed is emitted from a gas region that is approximately homogeneous in temperature and composition.

This assumption of "local thermodynamic equilibrium" is necessary when calculating temperatures using a Boltzmann distribution. The intensities of Al I spectral lines at wavelengths of 308.34, 309.44, 394.56, and 396.26 nm were used to calculate temperatures at different gate pulse delays according to the following equation:

$$\text{Ln}\,(I/(g_i A_{ki})) = -(E_k / kT) + \text{Ln}\,(C_\alpha F / U_\alpha(T)) , \qquad (8)$$

where I is the peak line intensity of atomic species α with concentration C_α, E_k is the upper energy level, T is the plasma temperature, $U_\alpha(T)$ is the partition function of the species α, k is the Boltzmann constant, F is a constant depending on experimental conditions, A_{ki} is the transition probability, and g_i is the statistical weight for the upper level. Spectroscopic data (table 1) were obtained from the National Institute of Standards and Technology database (*13*). A plot of Ln ($I / (g_i A_{ki})$) as a function of E_k will have a slope equal to –1/kT. A typical Boltzman plot using equation 8 is shown in figure 13.

Table 1. Spectroscopic parameters for Al I and Al II investigated lines.

	Wavelength (nm)	**A_{kj} (10^8 s^{-1})**	**E_k (eV)**	**g_i**	**ω (nm)**
Al I	308.34	0.63	4.021485	2	—
	309.44	0.74	4.021650	4	—
	394.56	0.49	3.142721	2	—
	396.26	0.98	3.142721	2	—
Al II	466.30	0.53	13.25646	3	6.85×10^{-3}
	747.14	0.94	15.30840	7	1.26×10^{-2}

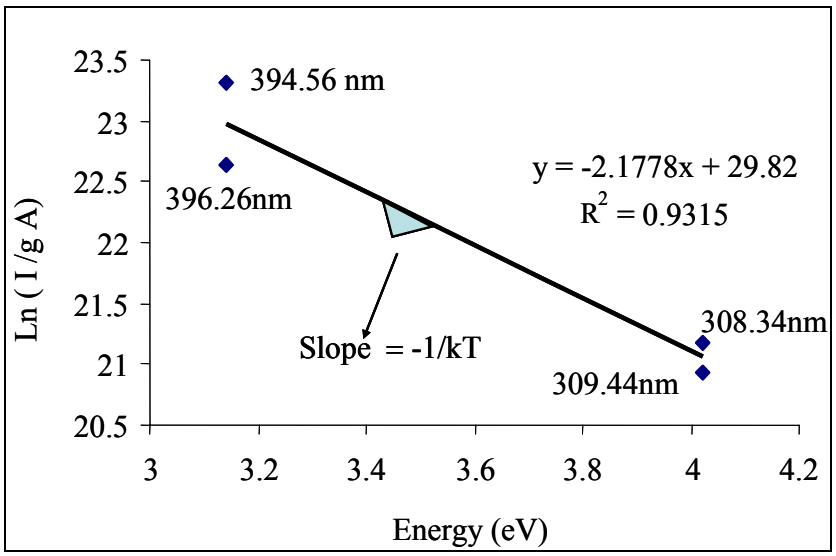

Figure 13. A Boltzman plot for 308.34-, 309.44-, 394.56-, and 396.26-nm Al I lines in O_2. The gate pulse width is 2 μs. The gate pulse delay is 15 μs.

Temperatures calculated using equation 8 and spectral line intensities from LIBS spectra measured in different bath gases are shown in figure 14. These calculated temperatures are in good agreement with previously reported calculated temperatures for similar systems (*14–16*). In general, the calculated temperature exhibits an approximately exponential decay over the emission lifetime.

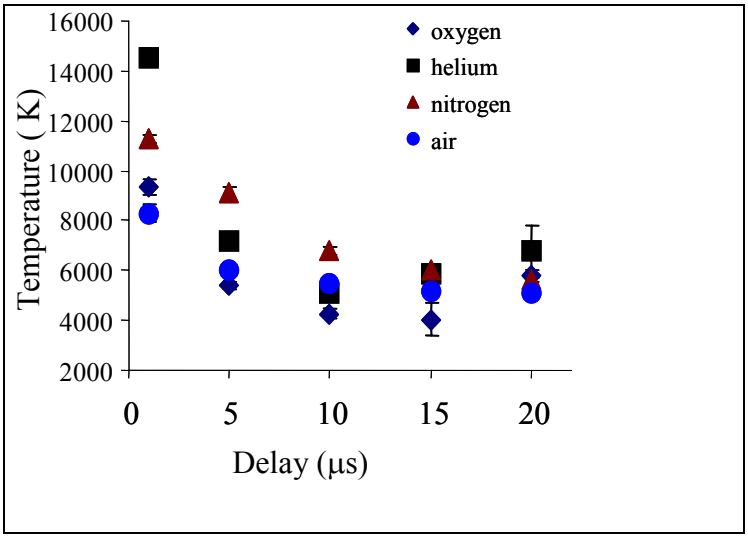

Figure 14. Excitation temperature vs. gate pulse delay with a 2-μs gate width.

3.4 Electron Density

The electron density (N_e) was determined using the Stark broadening effect (*17*) and assuming the plasma to be optically thin (negligible self absorption) for the Al II emission line at 747.14 nm. Stark broadening parameters are available for the lines at 747.14 and 466.3 nm (*18*). The Al II line at 466.3 nm was not used because this line is partially obscured by the AlO band near 484 nm. The relation between the line width (full width at half maximum [FWHM]) of the Stark broadened line and the electron density is given by equation 9:

$$\Delta\lambda_{1/2} = 2\omega\,(N_e / 10^{16}) + 3.5\,A\,(N_e / 10^{16})^{1/4}\;\;(1 - BN_D^{\,-1/3})\,\omega\,(N_e / 10^{16}), \qquad (9)$$

where $\Delta\lambda_{1/2}$ is the line width (FWHM), ω is the Stark broadening parameter, A is the ion broadening parameter, N_D is the number of particles in the Debye sphere, and B is a coefficient equal to 1.2 for ions and 0.75 for neutral lines. The values of ω were taken from Coloa et al. (*18*).

The measured line width was corrected to first order by subtracting the contribution of the instrumental line broadening. The instrument line broadening was found to be 0.1 nm, as determined by measuring the emission lines from a calibrated mercury lamp. The first term on the right side of equation 9 is the contribution of electron broadening. The second term on the

right side of equation 9 is the quasistatic ion broadening contribution, which can to be neglected in this analysis (*19*). Equation 9 then reduces to

$$\Delta\lambda_{1/2} = 2\omega\,(N_e / 10^{16}). \qquad (10)$$

In order to make a determination as to whether the local thermodynamic equilibrium conditions were satisfied for the selected spectral lines, the critical value of electron density distribution (N_e) was evaluated by following the procedure described by Aragon et al. (*20*). The critical limit of electron density distribution was determined from equation 11:

$$N_e \geq 1.6 \times 10^{12}\, T^{1/2}\,(E_k - E_i)^3\,. \qquad (11)$$

For the experiments reported here, the critical electron densities varied from 3×10^{15} to 9.5×10^{15} cm^{-3} for the temperature range from 4000 to 14,500 K. The lowest calculated electron density value exceeded these critical values by a factor of 20 for the range of temperatures calculated using the Boltzmann equation (equation 8). As seen in figure 15, there is a general trend toward lower electron densities at later decay times (also see figure 16) as the plasma cools.

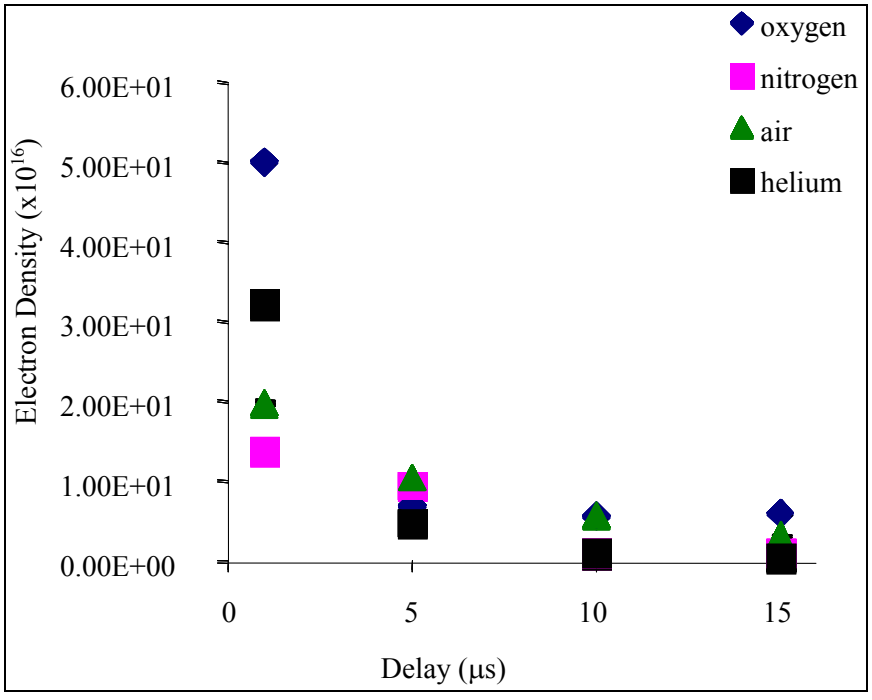

Figure 15. Electron density of Al vs. gate pulse delay with a 2-µs gate width.

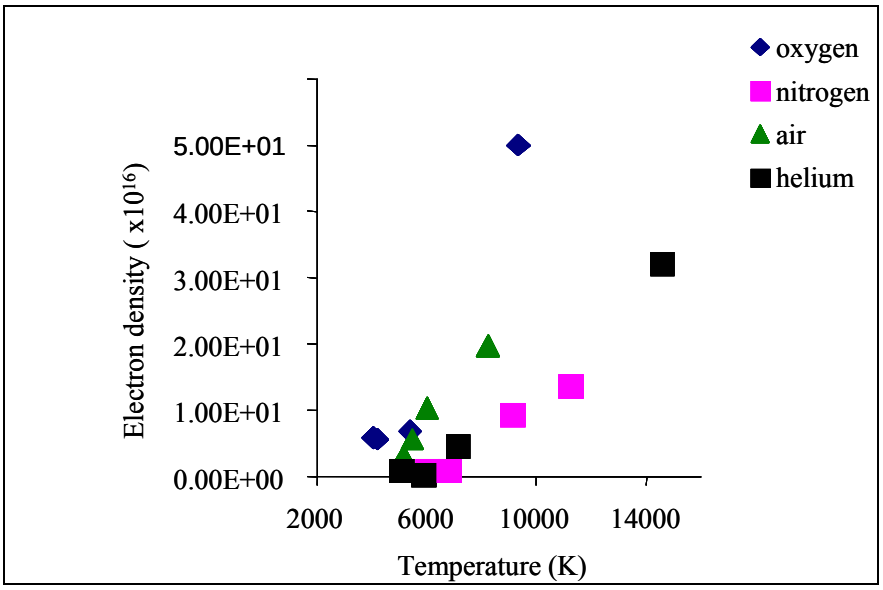

Figure 16. Excitation temperature vs. electron density profile in different atmospheres.

4. Conclusions

Measurements of the emission of AlO following exposure of an Al metal surface to a laser-induced spark have been carried out for bath gases of air, O_2, N_2, and He. Results of these experiments indicate that virtually all of the AlO emission is from AlO formed by the reaction of Al vapor with O_2 from the bath gas (if present). Emission from AlO initially present as an Al_2O_3 oxide layer on the metal sample was vanishingly small for emission spectra measured in bath gases of N_2 and He, when compared to the AlO emission measured in air and in O_2 bath gases. However, it is possible to distinguish the AlO emission from the Al_2O_3 oxide layer from AlO formed by reaction with ambient O_2 by examining the temporal behavior of the emission. The temporal behavior of Al and AlO emission following Al metal exposure to a laser-induced spark (in air and O_2) is consistent with known chemical mechanisms for Al combustion in O_2. Finally, calculations of temperature assuming a Boltzmann distribution of Al emission lines gives results in good agreement with calculations by previous investigators.

5. References

1. Brousseau, P.; Dorsett, H.; Cliff, M. Detonation Properties of Explosives Containing Nanometric Aluminum Powder in Microdetonics. *The Twelfth International Detonation Symposium*, San Diego, CA, 2002.

2. Mueller, D. C.; Turns, S. R. A Theoretical Evaluation of Secondary Atomization Effects on Engine Performance for Aluminum Gel Propellants. *J. Propulsion and Power* **1996**, *12*, 591–597.

3. Yuasa, S.; Zhu, Y.; Sogo, S. Ignition and Combustion of Aluminum in Oxygen/Nitrogen Mixture Streams. *Combustion and Flame* **1997**, *108*, 387–396.

4. Capitelli, F.; Coloa, F.; Provenzano, M. R.; Fantoni, R.; Brunetti, G.; Senesi, N. Determination of Heavy Metals in Soils by Laser-Induced Breakdown Spectroscopy. *Geoderma* **2002,** *106*, 45–62.

5. DeLucia, F. C., Jr.; Harmon, R. S.; McNesby, K. L.; Winkel, R. J., Jr.; Miziolek, A. W. Laser-Induced Breakdown Spectroscopy Analysis of Energetic Materials. *Appl. Opt. 42* **2003,** *30*, 6148.

6. Yueh, F. Y.; Sharma, R. C.; Singh, J. P.; Zhang, H.; Spencer, W. A. Evaluation of the Potential of Laser-Induced Breakdown Spectroscopy for Detection of Trace Element in Liquid. *J. Air Waste Manag. Assoc.* **2002**, *52* (11), 1307–15.

7. Portnov, A.; Rosenwaks, S.; Bar, I. Emission Following Laser-Induced Breakdown Spectroscopy of Organic Compounds in Ambient Air. *Appl. Opt*. **2003**, *42* (15), 2835–42.

8. Samuel, A. C.; DeLucia, F. C., Jr.; McNesby, K. L.; Miziolek, A. W. Laser-induced Breakdown Spectroscopy of Bacterial Spores, Molds, Pollens, and Protein: Initial Studies of Discrimination Potential. *Appl. Opt.* **2003**, *42* (30), 6205.

9. Simeonsson, J. B.; Miziolek, A. W. Time-Resolved Emission Studies of ArF Laser Produced Microplasmas. *Appl. Opt.* **1993**, *32* (6), 939–947.

10. Wainner, R. T.; Harmon, R. S.; Miziolek, A. W.; McNesby, K. L.; French, P. D. Analysis of Environmental Lead Contamination: Comparison of LIBS Field and Laboratory Instruments. *Spectrochemica Acta Part B* **2001**, *56* (6), 777–793.

11. Awadhesh, K. R.; Hansheng, Z.; Fang Yu, Y.; Singh, J. P.; Weisburg, A. Parametric Study of a Fiber-Optic Laser-Induced Breakdown Spectroscopy Probe for Analysis of Aluminum Alloys. *Spectrochimica Acta Part B* **2001**, *56* (12), 2371–2383.

12. Dokhan, A.; Price, E. W.; Seitzman, J. M.; Sigman, R. K. Combustion Mechanisms of Bimodal and Ultra Fine Aluminum in Ammonium Perchlorate Solid Propellant. *AIAA* **2002**, 4173.

13. National Institute of Standards and Technology Atomic Spectra Database Lines Form. http://physics.nist.gov/cgi-bin/AtData/lines_form (accessed 1 October 2004)

14. Le Drogoff, B.; Margot, J.; Chaker, M.; Sabsabi, M.; Barthelemy, O.; Johnston, T. W.; Laville, S.; Vidal, F.; Von Kaenel, Y. Temporal Characterization of Femtosecond Laser Pulses Induced Plasma for Spectrochemical Analysis of Aluminum Alloys. *Spectrochimica Acta Part B* **2001**, *56*, 987–1002.

15. Liu, H. C.; Mao, X. L.; Yoo, J. H.; Russo, R. E. Early Phase Laser Induced Plasma Diagnostic and Mass Removal During Single Pulse Laser Ablation of Silicon. *Spectrochimica Acta Part B* **1999**, *54*, 1607.

16. Amoruso, S. Modeling of UV-Pulsed Laser Ablation of Silicon. *Appl. Phys. A* **1999**, *69*, 323.

17. Saramdaev, E. V.; Salakhov, M. K. H. Regularities in the Stark Widths and Shifts of Spectral Lines of Singly-Ionized Aluminum. *J. Quant. Spectrsc. Radiat. Transfer* **1996**, *56* (3), 399–407.

18. Coloa, F.; Lazic, V.; Fantoni, F.; Pershin, S. A Comparison of Single and Double Pulse Laser-Induced Breakdown Spectroscopy of Aluminum Samples. *Spectrochimica Acta Part B* **2002**, *57*, 1167–1179.

19. Abdellatif, G.; Imam, H. A Study of the Laser Plasma Parameters at Different Laser Wavelengths. *Spectrochimica Acta Part B* **2002**, *57*, 1155–1165.

20. Aragon, C.; Bengoechea, J.; Aguilera, J. A. Influence of the Optical Depth on Spectral Line Emission From Laser-Induced Plasmas. *Spectrochimica Acta Part B* **2001**, *56*, 619.

NO. OF COPIES ORGANIZATION

1 (PDF ONLY) DEFENSE TECHNICAL INFORMATION CTR
DTIC OCA
8725 JOHN J KINGMAN RD
STE 0944
FORT BELVOIR VA 22060-6218

1 US ARMY RSRCH DEV & ENGRG CMD
SYSTEMS OF SYSTEMS INTEGRATION
AMSRD SS T
6000 6TH ST STE 100
FORT BELVOIR VA 22060-5608

1 INST FOR ADVNCD TCHNLGY
THE UNIV OF TEXAS
AT AUSTIN
3925 W BRAKER LN STE 400
AUSTIN TX 78759-5316

1 US MILITARY ACADEMY
MATH SCI CTR EXCELLENCE
MADN MATH
THAYER HALL
WEST POINT NY 10996-1786

1 DIRECTOR
US ARMY RESEARCH LAB
IMNE AD IM DR
2800 POWDER MILL RD
ADELPHI MD 20783-1197

3 DIRECTOR
US ARMY RESEARCH LAB
AMSRD ARL CI OK TL
2800 POWDER MILL RD
ADELPHI MD 20783-1197

3 DIRECTOR
US ARMY RESEARCH LAB
AMSRD ARL CS IS T
2800 POWDER MILL RD
ADELPHI MD 20783-1197

NO. OF COPIES ORGANIZATION

ABERDEEN PROVING GROUND

1 DIR USARL
AMSRD ARL CI OK TP (BLDG 4600)

NO. OF COPIES	ORGANIZATION
3	AIR FORCE RSCH LAB EDWARDS (AFRL) AFRL EDWARDS/USC ERC/AFRL K CRISTE 10 E SATURN BLVD EDWARDS AFB CA 93524
1	AIR FORCE RSCH LAB AFRL/PRSP BLDG 8451 G DRAKE 10 E SATURN BLVD EDWARDS AFB CA 93524
1	AIR FORCE RSCH LAB EGLIN (AFRL) AFRL/MNME W COOPER 2306 PERIMETER RD EGLIN AFB FL 32542
1	AIR FORCE RSCH LAB AFRL/MNME M FAJARDO 2306 PERIMETER RD EGLIN AFB FL 32542
1	AIR FORCE RSCH LAB AFRL/MNAV S FEDERLE 101 W EGLIN BLVD STE 342 EGLIN AFB FL 32542
1	AIR FORCE RSCH LAB AFRL/MN S KORN 101 W EGLIN BLVD STE 105 EGLIN AFB FL 32542-6810
1	AIR FORCE RSCH LAB AFRL/MNME M KRAMER 2306 PERIMETER RD EGLIN AFB FL 32542-6810
1	AIR FORCE RSCH LAB AFRL/MNAC J KUJALA 101 W EGLIN BLVD STE 334 EGLIN AFB FL 32542-6810
1	AIR FORCE RSCH LAB AFRL/MNME W R MAINES 2306 PERIMETER RD EGLIN AFB FL 32542
1	AIR FORCE RSCH LAB AFRL/MNME T MCKELVEY 2306 PERIMETER RD EGLIN AFB FL 32542-5910
1	AIR FORCE RSCH LAB AFRL/MNME D W RICHARDS 2306 PERIMETER RD EGLIN AFB FL 32542
1	AIR FORCE RSCH LAB AFRL/MNME C RUMCHIK 2306 PERIMETER RD EGLIN AFB FL 32542
1	AIR FORCE RSCH LAB AFRL/MNME L STEWART 2306 PERIMETER RD EGLIN AFB FL 32542
1	AIR FORCE RSCH LAB AFRL/MNME K WALKER 2306 PERIMETER RD EGLIN AFB FL 32542
1	AIR FORCE AFOSR M BERMAN AFOSR 4015 WILSON BLVD RM 713 ARLINGTON VA 22203-1954
1	US ARMY ARDEC/WECAC AMSTA AR WEE/B3022 D DOWNS PICATINNY ARSENAL NJ 07806-5000
1	US ARMY TACOM ARDEC P HAN BLDG 3022 PICATINNY ARSENAL NJ 07806-5000

NO. OF COPIES ORGANIZATION

1 US ARMY TACOM ARDEC
AMSTA AR WEE A
L HARRIS
PICATINNY ARSENAL NJ 07806

1 US ARMY TACOM ARDEC
AMSTA AR WEA BLDG 355
D KAPOOR
PICATINNY ARSENAL NJ 07806

1 US ARMY TACOM ARDEC
AMSTA AR WE BLDG 1
J LANNON
PICATINNY ARSENAL NJ 07806-5000

1 US ARMY TACOM ARDEC
AMSTA AR WEE/B3022
S NICOLICH
PICATINNY ARSENAL NJ 07806-5000

1 US ARMY TACOM ARDEC
R PAWLICKI
DOTC BLDG 3022 RM 222
PICATINNY ARSENAL NJ 07806-5000

1 US ARMY TACOM ARDEC
V STEPANOV
BLDG 3028
PICATINNY ARSENAL NJ 07806

1 US ARMY TACOM ARDEC
R SURAPANENI
BLDG 3022
PICATINNY ARSENAL NJ 07806-5000

1 CDR
US ARMY TACOM ARDEC
AMSTA AR WEE A
T VLADIMIROFF
PICATINNY ARSENAL NJ 07806

1 CDR US ARMY AMRDEC
US AVIATION AND
MISSILE CMD
AMSAM RD PS PT
R HATCHER
REDSTONE ARSENAL AL 35989

1 CDR US ARMY AMRDEC
US AVIATION AND
MISSILE CMD
AMSAM RD PS WF
S HILL
REDSTONE ARSENAL AL 35898-5247

NO. OF COPIES ORGANIZATION

1 CDR US ARMY AMRDEC
US AVIATION AND
MISSILE CMD
AMSAM RD PS WF
A STULTS
REDSTONE ARSENAL AL 5989-5247

1 CDR US ARMY AMRDEC
US AVIATION AND
MISSILE CMD
AMSAM RD PS PT BLDG 7120
D THOMPSON
REDSTONE ARSENAL AL 35989

1 US ARMY RSCH OFFICE
D MANN
PO BOX 12211
RSCH TRIANGLE PARK NC 27709-2211

1 NATL GROUND INTELLIGENCE CTR
IANG GS MT/MS 306
C BEITER
2055 BOULDER RD
CHARLOTTESVILLE VA 22911-8318

1 NATL GROUND INTELLIGENCE CTR
IANG GS MT/MS 306
R YOBS
2055 BOULDER RD
CHARLOTTESVILLE VA 22911-8318

1 CDR US ARMY SOLDIER SYSTEMS CTR
AMSSB RIP B (N)
M MAFFEO
NATICK MA 01760-5019

1 CDR US ARMY SOLDIER SYSTEMS CTR
AMSSB RIP B (N)
J WARD
NATICK MA 01760-5019

1 US ARMY SPECIAL OPERATIONS CMD
CAG COMBAT APPLICATIONS GROUP
L BOIVIN
PO BOX 70660
FT BRAGG NC 28307

NO. OF COPIES ORGANIZATION

1 US ARMY SPECIAL OPERATIONS CMD
CAG COMBAT APPLICATIONS GROUP
G GEORGEVITCH
PO BOX 71859
FT BRAGG NC 28307-5000

1 US ARMY SPECIAL OPERATIONS CMD
CAG COMBAT APPLICATIONS GROUP
D JETER
PO BOX 70660
FT BRAGG NC 28307

1 US MARINE CORPS
CTR FOR EMERGING THREATS AND OPPORTUNITIES
C CURCIO
3087 ROAN AVE BLDG 3087C
QUANTICO VA 22134

1 US MARINE CORPS
MARINE CORPS SYSTEMS CMD
CESS PM NBC DEFENSE MEDICAL
MCSC MED
T EAGLES
20333 BARNETT AVE STE 315
QUANTICO VA 22134-5010

1 NAVAL AIR WARFARE CTR
NAVAIR WEAPONS DIV
J BALDWIN
1 ADMINISTRATION CIRCLE
CODE 477200D
CHINA LAKE CA 93555-6100

1 NAVAL AIR WARFARE CTR
NAVAIR WEAPONS DIV
T BOGGS
CODE 4T4300D
CHINA LAKE CA 93555-6100

1 NAVAL AIR WARFARE CTR
NAVAIR WEAPONS DIV
CODE 4T4310D
M CHAN
CHINA LAKE CA 93555-6100

NO. OF COPIES ORGANIZATION

1 NAVAL AIR WARFARE CTR
NAVAIR WEAPONS DIV
CODE 4T4200D
R CHAPMAN
CHINA LAKE CA 93555-6100

1 NAVAL AIR WARFARE CTR
NAVAIR WEAPONS DIV
CODE 478400D
P DIXON
1 ADMINISTRATION CIRCLE
CHINA LAKE CA 93555-6100

1 NAVAL AIR WARFARE CTR
NAVAIR WEAPONS DIV
T FOLEY
1 ADMINISTRATION CIRCLE
CHINA LAKE CA 93555-6100

1 NAVAL AIR WARFARE CTR
NAVAIR WEAPONS DIV
K HIGA
1 ADMINISTRATION CIRCLE
CHINA LAKE CA 93555-6100

1 NAVAL AIR WARFARE CTR
NAVAIR WEAPONS DIV
CODE 477200D
B LORMAND
1 ADMINISTRATION CIRCLE
CHINA LAKE CA 93555-6100

1 NAVAL AIR WARFARE CTR
NAVAIR WEAPONS DIV
CODE 477200D
M MASON
1 ADMINISTRATION CIRCLE
CHINA LAKE CA 93555-6100

1 NAVAL AIR WARFARE CTR
NAVAIR WEAPONS DIV
CODE 4T4320D
T PARR
CHINA LAKE CA 93555-6100

1 NAVAL ORDNANCE SAFETY AND SECURITY ACTIVITY
D PORADA
23 STRAUSS AVE
INDIAN HEAD MD 20640

NO. OF COPIES ORGANIZATION

1 NAVAL ORDNANCE SAFETY AND SECURITY ACTIVITY
K TOMASELLO
FARAGUT HALL BLDG D323
23 STRAUSS AVE
INDIAN HEAD MD 20640-1541

1 US NAVAL RSCH LAB
CODE 6189
R MOWREY
4555 OVERLOOK AVE SW
WASHINGTON DC 20375-5342

1 US NAVAL RSCH LAB
CHEMISTRY DIV CODE 6125
J RUSSELL
4555 OVERLOOK AVE SW
WASHINGTON DC 20375-5342

1 CDR NAVAL SEA SYSTEMS CMD
INDIAN HEAD
CODE 910A
W KOPPES
101 STRAUSS AVE
INDIAN HEAD MD 20640-5035

1 CDR NAVAL SURFACE WARFARE CTR
CODE 4023 BLDG3347
S D'ARCHE
300 HWY 361
CRANE IN 47522-5001

1 NAVAL SURFACE WARFARE CTR
CODE G22 BLDG 221
R GARRETT
17320 DAHLGREN RD
DAHLGREN VA 22448-5100

1 NAVAL SURFACE WARFARE CTR
CODE G24
S HOCK
17320 DAHLGREN RD
DAHLGREN VA 22448-5100

1 NAVAL SURFACE WARFARE CTR
CODE G24
B KNOTT
17320 DAHLGREN RD
DAHLGREN VA 22448-5100

NO. OF COPIES ORGANIZATION

1 NAVAL SURFACE WARFARE CTR
E LACY
17320 DAHLGREN RD
DAHLGREN VA 22448-5100

1 NAVAL SURFACE WARFARE CTR
CODE G22
S WAGGENER
17320 DAHLGREN RD
DAHLGREN VA 22448-5100

1 NAVAL SURFACE WARFARE CTR
CODE 910 W BLDG 600
V BELLITTO
101 STRAUSS AVE
INDIAN HEAD MD 20640

1 NAVAL SURFACE WARFARE CTR
BLDG 600
J CAREY
101 STRAUSS AVE
INDIAN HEAD MD 20640

1 NAVAL SURFACE WARFARE CTR
CODE 440C
P CARPENTER
101 STRAUSS AVE
INDIAN HEAD MD 20640

1 NAVAL SURFACE WARFARE CTR
CODE 910F
J CHANG
101 STRAUSS AVE
INDIAN HEAD MD 20640

1 NAVAL SURFACE WARFARE CTR
D CICHRA
101 STRAUSS AVE
INDIAN HEAD MD 20640-5035

1 NAVAL SURFACE WARFARE CTR
EXPLOSIVES TEST & DEVELOPMENT
CODE 370
D COOK
101 STRAUSS AVE BLDG 695
INDIAN HEAD MD 20640

1 NAVAL SURFACE WARFARE CTR
R CRAMER
101 STRAUSS AVE
INDIAN HEAD MD 20640

NO. OF COPIES ORGANIZATION

1 NAVAL SURFACE WARFARE CTR
CODE 90D
R DOHERTY
101 STRAUSS AVE
INDIAN HEAD MD 20640-5035

1 NAVAL SURFACE WARFARE CTR
M DUNN
101 STRAUSS AVE BLDG 695
INDIAN HEAD MD 20640-5035

1 NAVAL SURFACE WARFARE CTR
CODE ST
A DUONG
101 STRAUSS AVE
INDIAN HEAD MD 20640-5035

1 NAVAL SURFACE WARFARE CTR
BLDG 600
F FOROHAR
101 STRAUSS AVE
INDIAN HEAD MD 20640-5035

1 NAVAL SURFACE WARFARE CTR
CODE 920J
R GUIRGUIS
101 STRAUSS AVE
INDIAN HEAD MD 20640-5035

1 NAVAL SURFACE WARFARE CTR
RSCH & TECHNOLOGY DEPT
CODE 9100 BLDG 600
J HARPER
101 STRAUSS AVE
INDIAN HEAD MD 20640-5035

1 NAVAL SURFACE WARFARE CTR
R JONES
101 STRAUSS AVE
INDIAN HEAD MD 20640

1 NAVAL SURFACE WARFARE CTR
ENERGETIC MATERIALS RSCH
CODE 920L BLDG 600
V JOSHI
101 STRAUSS AVE
INDIAN HEAD MD 20640-5035

1 NAVAL SURFACE WARFARE CTR
RSCH AND TECH DEPT
CODE 910R
R JOUET
101 STRAUSS AVE
INDIAN HEAD MD 20640-5035

NO. OF COPIES ORGANIZATION

1 NAVAL SURFACE WARFARE CTR
BLDG 490 ROOM 220
C KNOTT
101 STRAUSS AVE
INDIAN HEAD MD 20640

1 NAVAL SURFACE WARFARE CTR
BLDG 600
J MANNION
101 STRAUSS AVE
INDIAN HEAD MD 20640

1 NAVAL SURFACE WARFARE CTR
BLDG D 323 CODE 4210M
R MCCALL
101 STRAUSS AVE
INDIAN HEAD MD 20640

1 NAVAL SURFACE WARFARE CTR
CODE 90
P MILLER
101 STRAUSS AVE
INDIAN HEAD MD 20640

1 NAVAL SURFACE WARFARE CTR
CODE 920D BLDG 600
S MILLER
101 STRAUSS AVE
INDIAN HEAD MD 20640

1 NAVAL SURFACE WARFARE CTR
CODE 920
G PANGILINAN
101 STRAUSS AVE
INDIAN HEAD MD 20640

1 NAVAL SURFACE WARFARE CTR
CODE 920U BLDG 600
L PARKER
101 STRAUSS AVE
INDIAN HEAD MD 20640

1 NAVAL SURFACE WARFARE CTR
CODE 920P BLDG 600
S PEIRIS
101 STRAUSS AVE
INDIAN HEAD MD 20640

1 NAVAL SURFACE WARFARE CTR
D ROSENBERG
101 STRAUSS AVE
INDIAN HEAD MD 20640

NO. OF COPIES ORGANIZATION

1 NAVAL SURFACE WARFARE CTR
CODE 370JG BLDG 695
J ROGERSON
101 STRAUSS AVE
INDIAN HEAD MD 20640

1 NAVAL SURFACE WARFARE CTR
J SALAN
101 STRAUSS AVE
INDIAN HEAD MD 20640

1 NAVAL SURFACE WARFARE CTR
CODE CSE BLDG 600
A STERN
101 STRAUSS AVE
INDIAN HEAD MD 20640-5035

1 NAVAL SURFACE WARFARE CTR
CODE 4210D
C WALSH
101 STRAUSS AVE
INDIAN HEAD MD 20640

1 NAVAL SURFACE WARFARE CTR
INDIAN HEAD
CODE 910X BLDG 600
A WARREN
101 STRAUSS AVE
INDIAN HEAD MD 20640

1 OFFICE OF NAVAL RSCH
C BEDFORD
800 N QUINCY ST
ARLINGTON VA 22217

1 NAVAL AIR SYSTEMS CMD
PATUXENT (NAVAIR)
HQ AIR 4 7
48150 SHAW RD BLDG 2109 RM 122
A GEHRIS
PATUXENT RIVER MD 20670

1 OFFICE OF SECRETARY OF DEFENSE
ODUSD/S&T
1777 N KENT ST STE 9030
D TAM
ARLINGTON VA 22209

NO. OF COPIES ORGANIZATION

1 PENTAGON
LW&M LAND WARFARE & MUNITIONS
D BAUM
OUSD(AT&L)/DS/LW&M RM 3B1060
3090 DEFENSE PENTAGON
WASHINGTON DC 20301-3090

1 OUSD(AT&L)/DS/LAND WARFARE & MUNITIONS
S ROJAS
RM 3B1060
3090 DEFENSE PENTAGON
WASHINGTON DC 20301-3090

1 ARGONNE NATL LAB
K CARNEY
PO BOX 2528
IDAHO FALLS ID 83404

1 ARGONNE NATL LAB
CHEMISTRY DIVISION
J HESSLER
9700 SOUTH CASS AVE
ARGONNE IL 60439-4831

1 LAWRENCE LIVERMORE NATL LAB
PO BOX 808 L 092
A GASH
LIVERMORE CA 94551

1 LAWRENCE LIVERMORE NATL LAB
MS L 30
A KUHL
PO BOX 808
LIVERMORE CA 94550

1 LAWRENCE LIVERMORE NATL LAB
L 282
J MOLITORIS
PO BOX 808
LIVERMORE CA 94551

1 LOS ALAMOS NATL LAB
MS P918 DX DO
W DANEN
LOS ALAMOS NM 87545

NO. OF COPIES ORGANIZATION

1 LOS ALAMOS NATL LAB
MS E549
K HUBBARD
LOS ALAMOS NM 87545

1 LOS ALAMOS NATL LAB
MS C920
S SON
LOS ALAMOS NM 87545

1 LOS ALAMOS NATL LAB
GROUP DX 2 MS C920
B TAPPAN
LOS ALAMOS NM 87545

1 SANDIA NATL LABORATORIES
MS 0836
M BAER
ALBUQUERQUE NM 87185-0836

1 SANDIA NATL LABORATORIES
MS 0836
E HERTEL
ALBUQUERQUE NM 87185-0836

1 SANDIA NATL LABORATORIES
MS 1172
T HITCHCOCK
PO BOX 5800
ALBUQUERQUE NM 87185-1172

1 SANDIA NATL LABORATORIES
PO BOX 5800
MS 1452
B INGRAM
ALBUQUERQUE NM 87185-1452

1 SANDIA NATL LABORATORIES
PO BOX 5800 MS 1454
M KANESHIGE
ALBUQUERQUE NM 87185-1454

1 SANDIA NATL LABORATORIES
PO BOX 5800 MS 1452
B MELOF
ALBUQUERQUE NM 87185-1452

1 SANDIA NATL LABORATORIES
PO BOX 5800 MS 1454
A RENLUND
ALBUQUERQUE NM 87185-1424

NO. OF COPIES ORGANIZATION

1 DEFENSE THREAT
REDUCTION AGENCY
TDSH J KOLTS
STOP 6201
8725 JOHN J KINGMAN RD
FORT BELVOIR VA 22060

1 DCI CTR FOR WEAPONS
INTELLIGENCE
NONPROLIFERATION AND
ARMS CONTROL
WINPAC
M AGUILO
WASHINGTON DC 20505

1 J BACKOFEN
2668 PETERSBOROUGH ST
HERNDON VA 20171-2443

1 C LLOYD
47110 SOUTHAMPTON
STERLING VA 20165

1 DCI CTR FOR WEAPONS
INTELLIGENCE
NONPROLIFERATION AND
ARMS CONTROL WINPAC
J WALTON
WASHINGTON DC 20505

1 DEFENSE INTELLIGENCE
AGENCY
BLDG 6000 DWO 4
K CRELLING
BOLLING AIR FORCE BASE
WASHINGTON DC 20340-5100

1 AEROJET
E LIU
PO BOX 13222
SACRAMENTO CA 95813

1 ALLIANT TECHSYSTEMS INC
C ZISETTE
PO BOX 1
RADFORD VA 24141

1 APPLIED RSCH ASSOCIATES
C NEEDHAM
SUITE A 220
4300 SAN MATEO BLVD NE
ALBUQUERQUE NM 87110

NO. OF COPIES	ORGANIZATION
1	ARGONIDE CORP F TEPPER 291 POWER CT SANFORD FL 32771
1	ATK THIOKOL PROPULSION PO BOX 707 MS 244 J AKESTER BRIGHAM CITY UT 84302-0707
1	ATK THIOKOL PROPULSION PO BOX 707 MS 244 P BRAITHWAITE BRIGHAM CITY UT 84302
1	ATK THIOKOL PROPULSION PO BOX 707 MS 230 S GLAITTLI BRIGHAM CITY UT 84302-0707
1	ATK THIOKOL PROPULSION PO BOX 707 MS 244 K LEE BRIGHAM CITY UT 84302-0707
1	ATK THIOKOL PROPULSION PO BOX 707 MS 244 G LUND BRIGHAM CITY UTAH 84302
1	ATK THIOKOL PROPULSION PO BOX 707 MS 230 S LUSK BRIGHAM CITY UT 84302-0707
1	BATTELLE MEMORIAL INSTITUTE T BURKY 505 KING AVE COLUMBUS OH 43201
1	BOOZ ALLEN HAMILTON G ZUCCARELLO 3811 N FAIRFAX DR STE 600 ARLINGTON VA 22203
1	CACI INC M EGGLESTON 14151 PARK MEADOW DR CHANTILLY VA 20151
1	DE TECHNOLOGIES INC C FORSYTH 3620 HORIZON DR KING OF PRUSSIA PA 19406
1	ENERGETIC MATERIALS APPLICATIONS L JOSEPHSON 300 DAWN CT RIDGECREST CA 93555
1	ENSIGN BICKFORD AEROSPACE & DEFENSE A GARVEY 640 HOPMEADOW ST BLDG 46 SIMSBURY CT 06070
1	EXOTHERM CORPORATION A LASCHIVER 1035 LINE ST CAMDEN NJ 08103
1	GENERAL SCIENCES INC P ZAVITSANOS 205 SCHOOLHOUSE RD SOUDERTON PA 18964
1	GEO CTRS INC BLDG 3028 D PARITOSH PICATINNY ARSENAL NJ 07806-5000
1	HICKS & ASSOCIATES INC SUITE 1300 C KITCHENS JR 1710 SAIC DR MCLEAN VA 22102
1	NANOTECHNOLOGIES INC D HAMILL 1908 KRAMER LN AUSTIN TX 78758
1	NORTHROP GRUMMAN CORP/DTRA J COCCHIARO 6940 S KINGS HIGHWAY STE 210 ALEXANDRIA VA 22310
1	NORTHROP GRUMMAN IT M SEIZEW PO BOX 471 SAN PEDRO CA 90733-0471
1	PRATT & WHITNEY N TRIVEDI 600 METCALF RD SAN JOSE CA 95138

NO. OF
COPIES ORGANIZATION

1 ST MARKS POWDER
A GENERAL DYNAMICS CO
J DRUMMOND
PO BOX 222
ST MARKS FL 32355

1 SAIC
W WAESCHE
4319 BANBURY DR
GAINESVILLE VA 20155

1 SRI INTERNATL
J BOTTARO
RM PS 318
333 RAVENSWOOD AVE
MENLO PARK CA 94025

1 TALLEY DEFENSE SYSTEMS
G KNOWLTON
40512 N HIGLEY RD
MESA AZ 85205

ABERDEEN PROVING GROUND

26 DIR USARL
AMSRD ARL WM B
A HORST
AMSRD ARL WM BD
W ANDERSON
R BEYER
A BRANT
S BUNTE
E BYRD
L CHANG
J COLBURN
P CONROY
B FORCH
B HOMAN
P KASTE
A KOTLAR
C LEVERITT
K MCNESBY
M MCQUAID
A MIZIOLEK
M NUSCA
R PESCE-RODRIGUEZ
B RICE
R SAUSA
AMSRD ARL WM TB
P BAKER
D KOOKER
B KRZEWINSKI
R LOTTERO
B ROOS